Indian Journal of Chemical Technology
Vol. 28, September 2021, pp. 572-579

Efficient sensing of resorcinol using onion peel derived carbon and barium titanate nanocomposite

E Murugan*, S Saranya, K Janakiraman & Greeshma Caroline Titus

Department of Physical Chemistry, School of Chemical Sciences, University of Madras, Guindy Campus, Chennai-600 025, Tamil Nadu, India

E-mail: dr.e.murugan@gmail.com

Received 18 March 2021; accepted 1 September 2021

A novel voltammetric sensor, Ag@$BaTiO_3$/rCF/GCE has been designed based on silver nanoparticle (AgNPs), barium titanate ($BaTiO_3$) and bio-inspired carbon derived from onion peel (OP) for the electrochemical determination of an organic pollutant, resorcinol (RS). The nanocomposite has been synthesized by ultrasonic irradiation of $BaTiO_3$ decorated on reduced carbon flakes (rCF) on which the Ag nanoparticles (AgNPs) are stabilized. It has been characterized by spectroscopic and microscopic techniques and Impedence spectroscopy. Its electrochemical activity is studied by the surface modification of the glassy carbon electrode (GCE) through cyclic voltammetry (CV) and differential pulse voltammetry (DPV). The results show a considerable decrease in the Rct equal to 239Ω which confirms the surface modification of the electrode. The slope value 0.7814 confirms that the electrocatalytic oxidation of RS is a typical adsorption-controlled process. The linear concentration range of resorcinol detection varies from 6.66 to 131.67 μM with a LOD of 0.378 μM.

Keywords: Cyclic voltammetry, Electrochemical sensor, Onion peel, Reduced carbon flakes (rCF), Silver nanoparticles, Ultrasonic irradiation

Carbon materials from culinary wastes have attracted considerable attention of researchers for the past two decades. Especially, carbon derived from onion peel has been exploited extensively in variety of applications owing to their novel structure, and several remarkable mechanical, thermal and electrical[1] properties. It is must to highlight that the basic structural unit of carbon resembles graphene sheet layers[2] separated as carbon flakes. An extensive literature survey reveals that the carbon flakes have enriched quantity of univalent anions and cations, and on calcination of onion peels leads to produce graphene structural based carbonaceous material[3]. Owing to its excellent electrical properties at room temperature, mechanical[4] and chemical stability[5], and ease of synthesis, $BaTiO_3$[6] has been decorated on OP to enhance the electrical conductivity[7]. Further, silver nanoparticles[8] were stabilized onto the surface of $BaTiO_3$ decorated OP in order to increase the reactive sites. It is in this background, it was planned to prepare electrochemically active carbonaceous materials for the modification of glassy carbon electrode for the electrochemical detection of resorcinol[9].

The chemical modification of the reduced carbon flakes surface was performed through reduction with hydrazine hydrate. rCF is expected to play a crucial role in tailoring the properties of the material after reduction of functional groups attached to the surface[10]. Hence, it reacts readily with other chemical reagent and form homogeneous dispersions. In the electrocatalytic reactions, it has been found that the catalytic activity of Ag@$BaTiO_3$/rCF nanocomposites depends mainly on the decoration of $BaTiO_3$ on the surface of the reduced rCF. Electrochemical determination of RS[11] is considered important, as it is highly toxic and a obstinate pollutant in the aqueous environment. It is a greater challenge to determine resorcinol from water samples. To overcome the challenge, it has been reported by H. Zhang *et al*. (2015) the values of recovery of resorcinol range from 91.7 to 107.7% from the tap water samples. Electrochemical detection of RS with various electrodes including carbon fiber electrode[12], carbon paste electrode[13] was reported. It was decided to fabricate an efficient electrode using graphene structure based components possessing enhanced electrical and chemical properties. To the best of our knowledge there is no study for the investigation of the electrochemical detection of RS using carbon derived from OP decorated with $BaTiO_3$ and silver nanoparticles.

Experimental Section

Barium hydroxide and titanium tetra butoxide were supplied by Sigma Aldrich. Disodium hydrogen phosphate and sodium dihydrogen phosphate were purchased from Sigma- Aldrich. Hydrazine hydrate from SRL and ethanol from SRL were used as received. Double distilled water was used for the preparation of various solutions.

Synthesis of rCF and $BaTiO_3$/rCF

Carbon material was obtained from onion peel (OP) by calcination at 400°C. Then it was reduced by hydrazine hydrate to obtain reduced carbon flakes (rCF). Perovskite - type $BaTiO_3$ nanoparticles were decorated on rCF by the ultrasonic - irradiation technique[14]. In a typical synthesis, Ti $(OBu)_4$ (0.2 mol) was dissolved in ethanol (25 mL) under vigorous stirring at 40°C to form a yellow solution. Then, $Ba(OH)_2 \cdot 8H_2O$ (0.05 M) was added to it. After 20 min, double distilled water (40 mL) was added to it which resulted in a milky white suspension. To the above suspension rCF (30 mg) was added and allowed to stir for 2 h. The product was separated by centrifugation at 5000 rpm and washed several times with ethanol and deionized water. Finally, the $BaTiO_3$/rCF nanocomposite was dried under a vacuum at 75°C for 24 h. For the synthesis of $BaTiO_3$ nanoparticles, the same procedure was followed without rCF.

Synthesis of Ag@$BaTiO_3$/rCF

$BaTiO_3$/rCF (0.1 g), was taken in a 100 mL round bottom flask containing 20 mL of dried ethanol. Aqueous solution of $AgNO_3$ (1.5 mM) 10 mL was added to it and stirred vigorously at 30°C for 3 h (Scheme 1). The obtained solid was washed twice with 5mL of deionized H_2O, 3 mL of acetone and 3mL of carbinol. Freshly prepared $NaBH_4$ (20 mM) solution 1 mL was slowly added to it drop by drop and the stirring was continued for 1 h[15]. The colour of the solution turned dark yellow and then to wine red after the final addition, indicating the formation of AgNPs stabilized on $BaTiO_3$/rCF denoted as Ag@$BaTiO_3$/rCF.

Fabrication of Ag@$BaTiO_3$/rCF coated GCE

Prior to modification, the nanocomposite was dispersed in ethanol (1 mg/mL) by ultra sonication. Then, the dispersed solution, about 5 µL, was drop cast onto the GCE surface and resulting $BaTiO_3$/rCF modified GCE was dried at room temperature (Scheme 1). Finally, the fabricated GCE was applied for the electrochemical determination of resorcinol. The stock solution of resorcinol (RS) (1mM) was prepared by dissolving 0.0011 g of it in 0.1M (*p*H 7.0) phosphate buffer solution (PBS), and it was stored in a refrigerator at 4°C. This stock solution was diluted to required concentrations as and when needed.

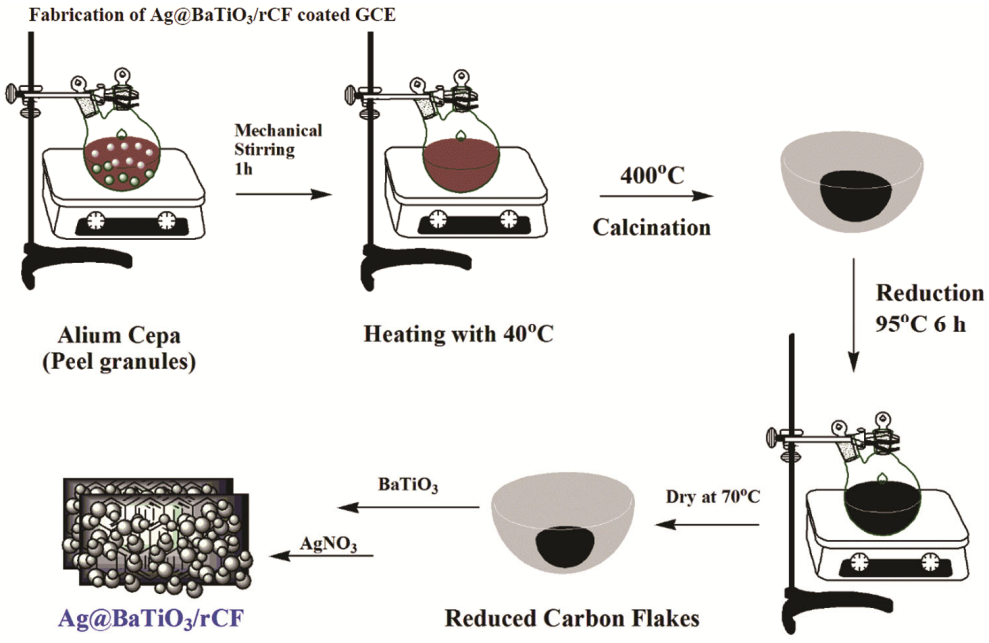

Scheme 1 — Synthesis of Ag@$BaTiO_3$/rCF

Results and Discussion

The characteristic reflections of rCF showed a broad diffraction peak at 16.5° (2θ) due to (001), and the peak at 22.4° (002), 43.13° (100) are assigned to aromatic carbon sheets[16] oriented in a relatively aligned manner (Fig. 1a). Generally free rCF yields a peak close to 10°C (2θ), but, here, in the spectra the peak positions have been shifted to higher angles. $BaTiO_3$ showed peaks at 22.29°, 31.53°, 38.92°, 45.06/45.31°, 50.87°, 56.34°, 65.93°, 70.48°, 75.03° and 79.44° (2θ) due to reflections from (100), (110), (111), (002)/(200), (102), (211), (220), (212), (310) and (311) respectively[17]. The peak splitting at approximately (2θ =) 45° $BaTiO_3$ (Fig. 1b) is attributed to tetragonal $BaTiO_3$ (JCPDS No. 01-075-0583) with a lattice parameter, a = b = 3.9950 Å, c = 4.0340 Å. The XRD patterns of $BaTiO_3$ nanoparticles and Ag@$BaTiO_3$/rCF (Fig. 1c) nanocomposite correlated well with the reported data of tetragonal phase of $BaTiO_3$ (JCPDS No. 01-075-0583) with a = 3.992 A°, c = 4.025 A° without any impurity phase.

FTIR analysis

The FT-IR spectrum of rCF (Fig. 2a) indicated the presence of various functional groups. The bands at 3413, 2965, 1730, 1630 and 1045 (Ref.18), correspond to the abundantly available organic residues such as O–H groups, CH_2, C=O, aromatic C=C and C–O–C groups, respectively. These observations suggest that the carbon flakes are abundant in oxygen. Such functional groups can participate in the formation and growth of $BaTiO_3$ on the rCF surface. The FT-IR spectrum (Fig. 2b) of the $BaTiO_3$ nanoparticles on rCF, yielded the bands at 3411 and 1630 cm^{-1} reveal broad H-O-H stretching and an O-H bending respectively. The peak at 1393 cm^{-1} is related to the stretching vibration of CO_3^{2-} due to the traces of $BaCO_3$ phase (less than 2.0 wt.%), and the broad band at 599 cm^{-1} is due to Ti - O (Ref. 19) stretching mode of $BaTiO_3$. After the growth of $BaTiO_3$ nanoparticles on rCF (Fig. 2c), the characteristic peaks at 836.18, 1621 and 3501.70 cm^{-1} showed the decoration of $BaTiO_3$ on rCF.

Raman spectral analysis

The Raman spectra of rCF (Fig. 3A) showed two peaks at approximately 1373 and 1563 cm^{-1}, which are the D-band and G-band, respectively. The G-band peak around 1563 cm^{-1} is characteristic of rCF corresponding to a well-defined sp^2 carbon-type structure, which can be attributed to the doubly degenerate mode. The D-band at approximately 1373 cm^{-1} can be attributed to the presence of defects or edges within the rCF composites, as shown in Fig. 3b. Peaks at 148, 407, 513 and 637 cm^{-1} [Ref. 20] were observed in the Raman spectra of

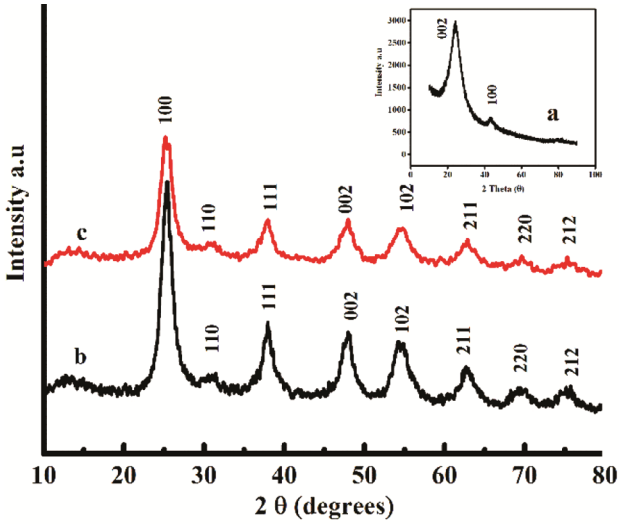

Fig. 1 — X-Ray diffraction pattern of (a) rCF,(b) $BaTiO_3$, and (c) Ag@$BaTiO_3$/rCF

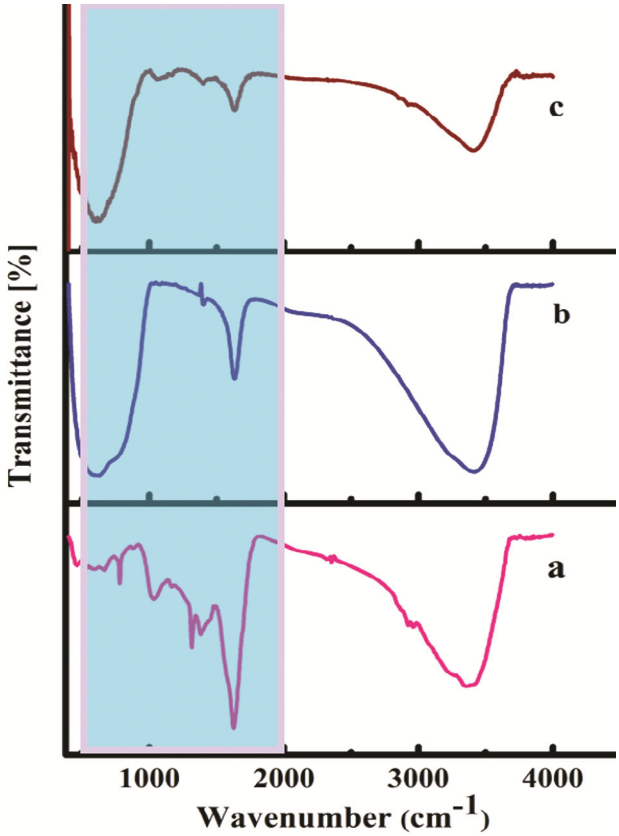

Fig. 2 — FT – IR spectrum of (a) rCF, (b) $BaTiO_3$ and (c) Ag@$BaTiO_3$/rCF

pure $BaTiO_3$ and the $BaTiO_3$/Rcf (Fig. 3C) nanocomposite. The existence of rCF in the composites is confirmed. The increase in intensity of the peaks observed for $BaTiO_3$/rCF confirms the decoration of $BaTiO_3$ on rCF. The characteristic peak of rCF inclined to migrate slightly to a lower frequency. The results indicated the absence of defects in the composites and many oxygen-containing functional groups were reduced during the hydrothermal process.

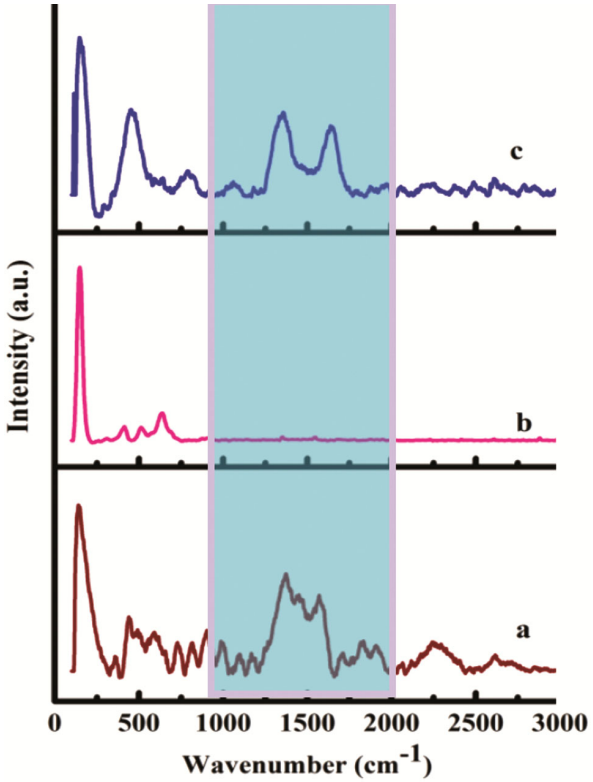

Fig. 3 — RAMAN spectrum for (a) rCF, (b) $BaTiO_3$ and (c) Ag@$BaTiO_3$/rCF

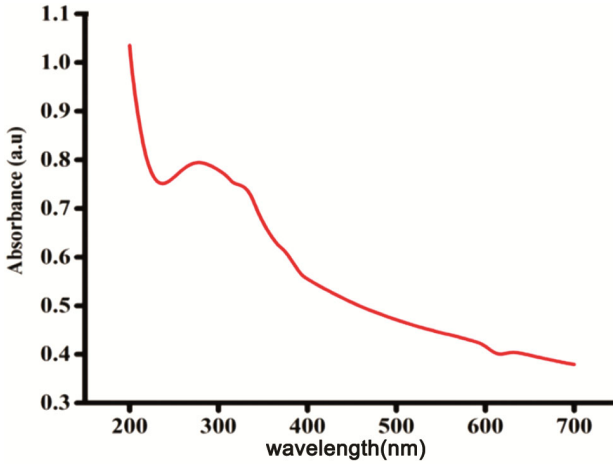

Fig. 4 — UV - Vis spectrum of Ag@$BaTiO_3$/rCF

UV – Visible spectral analysis

In the UV-Visible absorption spectra (Fig. 4), the absorption peak of rCF shifts to the wavelength around 278 nm, implying the deoxygenation of carbon flakes through reduction. The peak at 390 nm for Ag@$BaTiO_3$/rCF nanocomposite correspond to surface plasmons of AgNPs deposited on $BaTiO_3$/rCF surface.

HRSEM Analysis

In the HRSEM image of rCF flake like structure was noticed (Fig. 5A). The HRSEM image of barium titanate exhibited the sphere shaped granules, are aggregated together into a large spherical mass (Fig. 5B). The $BaTiO_3$ granules[21] and silver nanoparticles are decorated on the carbon flakes (Fig. 5C). This confirms the decoration of AgNPs and $BaTiO_3$ on the reduced carbon flakes.

EDAX Analysis

The EDAX spectrum of rCF showed presence of carbon and oxygen (Fig. 6A). The EDAX spectrum of $BaTiO_3$ showed an intense peak due to Ba, Ti and elemental oxygen which confirms the presence of $BaTiO_3$ (Fig. 6B). The presence of metallic AgNPs is confirmed by the presence of a strong peak at 3keV which is due to surface plasmon resonance (Fig. 6C).

Catalytic activity of Ag@$BaTiO_3$/rCF for the electrochemical oxidation of dopamine Hhydrochloride

Electrochemical characterization of surface modified electrodes

Impedance spectroscopy is considered important for probing the interfacial electron transfer resistance of all the surface modified electrodes using phosphate buffered saline (0.1M PBS). EIS was performed to monitor the changes of charge transfer resistance (Rct) that triggered from every surface modification step as shown in (Fig. 7). The charge transfer

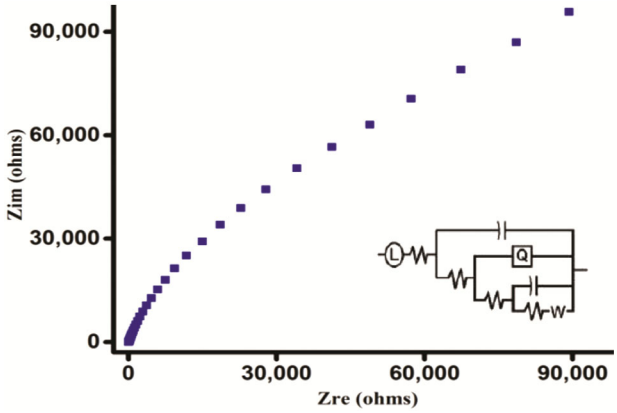

Fig. 5 — EIS spectrum of Ag@$BaTiO_3$/rCFin 0.1 M PBS LR(C(R(Q(R(C(RW)))))) (Fitted to Randles equivalent circuit)

resistance (Rct) of the modified electrode depends on dielectric and insulating features at the electrode/electrolyte interface[22]. The Rct value for the GCE modified Ag@$BaTiO_3$/rCF was equal to 239Ω. The low Rct value confirms the modification of the electrode and has the conducting behaviour. The Rct values of all the modified electrodes were fitted to Randles equivalent circuit.

Electrochemical detection of resorcinol

Electrochemical detection of resorcinol was performed using a Ag@$BaTiO_3$/rCF modified glassy carbon electrode (GCE). For this purpose, cyclic voltammetric (CV) and differential pulse voltammetric (DPV) techniques were applied using various *p*Hs 5.8-8.0 maintained with phosphate buffered saline (PBS). The response of the different modified electrode with and without RS at *p*H 5.8 is shown in (Fig. 8). The oxidation current of RS on Ag@$BaTiO_3$/rCF modified GCE was higher than that of Ag@$BaTiO_3$/rCF without RS, indicating that Ag@$BaTiO_3$/rCF is obviously catalytically active towards the RS oxidation (Scheme 2).

Optimization of the modified electrode Ag@$BaTiO_3$/rCF

The electrochemical behaviour of resorcinol at various *p*Hs (5.8 to 8.0) was studied at Ag@$BaTiO_3$/rCF shown in (Fig. 9). The oxidation potential increased with increase in *p*H from 5.8 to 8.0. High current was observed at the *p*H 5.8 at a lower potential of 0.6V. The Nernstian slope of -77 mV for Ag@$BaTiO_3$/rCF confirms the reaction of RS does not proceed through an equal number of proton and electron transfer. The anodic peak potential was shifted to the negative value with the increase in *p*H. The plot for Epa vs. *p*H in 0.1 M PBS yielded a linear regression equation

$E^{o}_{1/2}$ (mV) = -77 + 1.2431 (correlation coefficient $\gamma = 0.9432$) … (1)

Effect of frequency

The effect of frequency on the electrochemical behaviour of RS at Ag@$BaTiO_3$/rCF was studied by SWV. The square wave voltammograms of Ag@$BaTiO_3$/rCF in 0.1M PBS (*p*H 5.8) containing 1mM RS with frequency increased from 5 to 80 mVs^{-1} are shown in (Fig. 10A). The anodic peak current increased, as the frequency was increased as shown in (Fig. 10B). The linear relation between the log f and log current is illustrated in (Fig. 10C). The slope value of 0.7814 reveal that the process is adsorption controlled. The linear relationship of a double

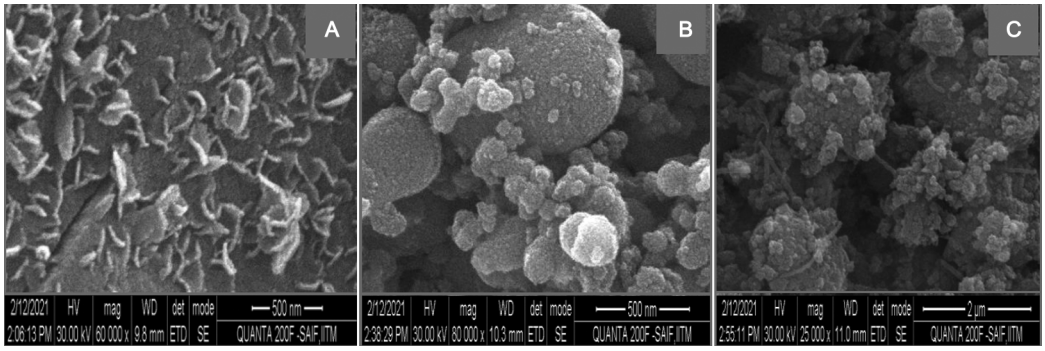

Fig. 6 — HRSEM image of (a) rCF, (b) $BaTiO_3$, and (c) Ag@$BaTiO_3$/rCF

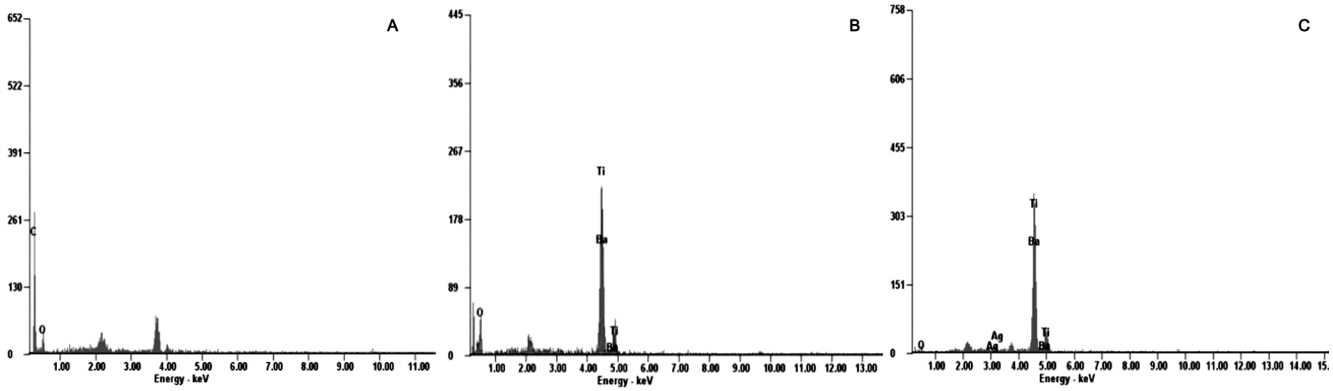

Fig. 7 — EDAX spectrum of (a) rCF(b) $BaTiO_3$, and (c) Ag@$BaTiO_3$/rCF

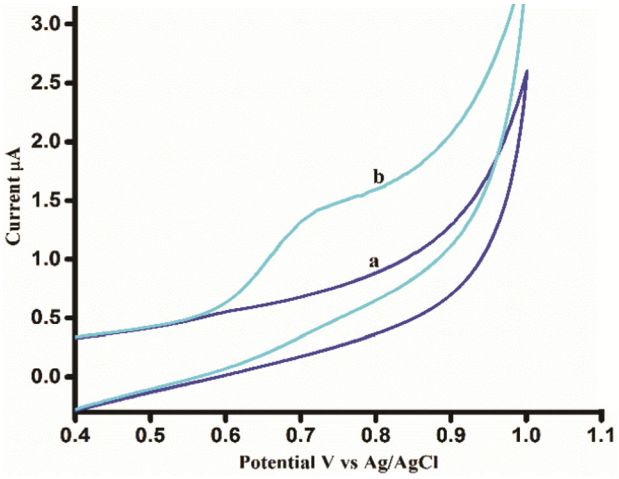

Fig. 8 — Cyclic Voltammograms of (a) Ag@$BaTiO_3$/rCF/GCE and (b) 1mM RS at Ag@$BaTiO_3$/rCF/GCE. Scan Rate: 50mV/s (PBS = 0.1M, *p*H = 5.8)

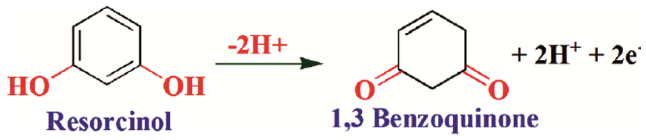

Scheme 2 — Electrochemical oxidation of resorcinol

logarithmic plot between frequency and peak current also supported that the process is adsorption controlled.

The linear regression equation is given below

$$I_{pa} = 1.8481\times 10^{-7} (v^{1/2}) + 2.1087 \times 10^{-6} (R^2 = 0.9824 \quad \ldots (2)$$

Determination of RS by DPV at Ag@$BaTiO_3$/rCF/GCE

With the experimental parameters obtained before, we further examined the application of our modified electrode (Ag@$BaTiO_3$/rCF/GCE) using differential pulse voltammogram. (Fig. 11A) represents the differential pulse voltammograms of RS at 1mM in which no peak current was observed for bare GCE. This suggests the poor electrochemical behaviour and so the modified Ag@$BaTiO_3$/rCF/GCE electrode showed an irreversible anodic peak (Epa) at 0.6 V. The oxidation current increased with the increasing concentration of resorcinol at a linear concentration range of 6.66-131.67 µM with a LOD of 0.38 µM. The limit of quantification (LOQ) was observed to be 0.0013 µM with a sensitivity of 0.0072 µA/Mm. Comparison of performance of the

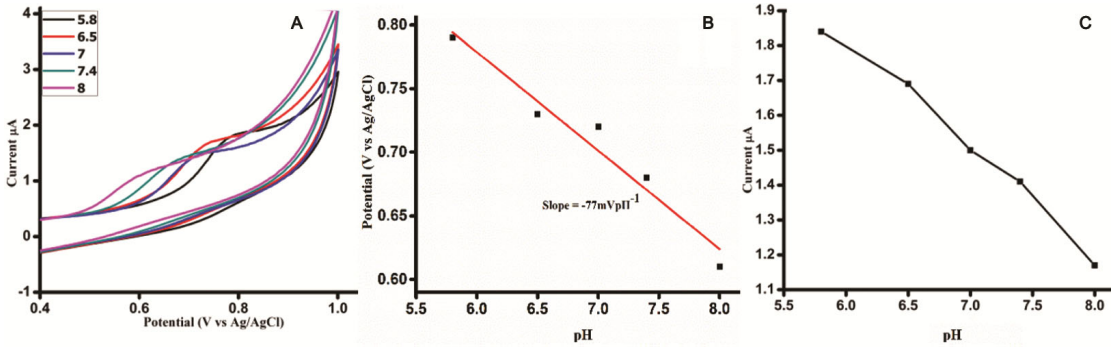

Fig. 9 — (A) Cyclic Voltammograms of oxidation of RS in 0.1 M PBS at different *p*Hs with Ag@$BaTiO_3$/rCF/GCE,(B) Plot of $E_{1/2}$ of DH vs. *p*H value and (C) Plot of *p*H vs. peak current

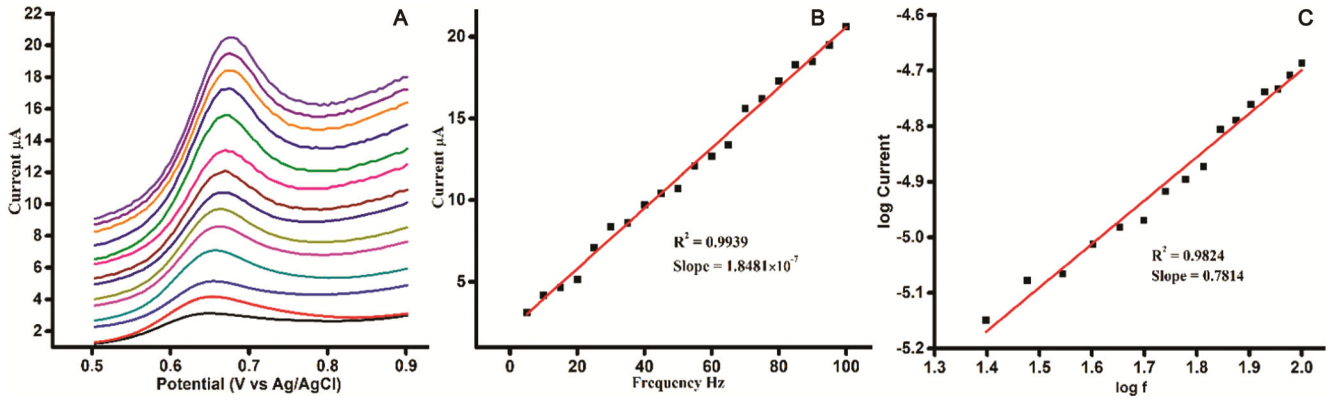

Fig. 10 — (A) Square wave voltammograms for the oxidation of resorcinol (0.10 M PBS, *p*H = 5.8; (B) Effect of frequency vs peak current at Ag@$BaTiO_3$/rCF/GCE and (C) Double logarithmic plot of log f vs. log current

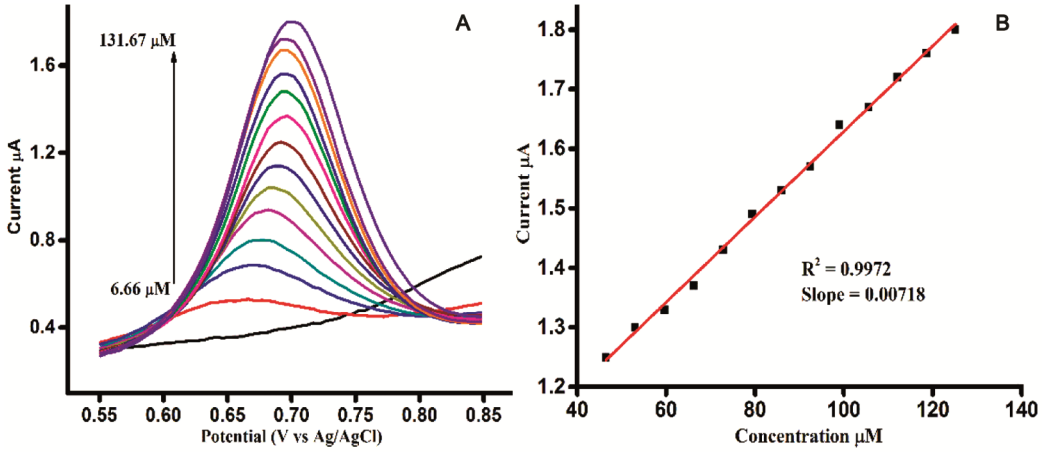

Fig. 11 — (A) Differential pulse voltammograms of oxidation of RS in 0.1M PBS with Ag@$BaTiO_3$/rCF/GCE at different concentrations at a scan rate of 50mVs^{-1} (B) Calibration plot for concentration of RS vs. Current

Table 1 — Comparison of performance of the fabricated electrode for RS detection with other electrodes

Electrode	Linear Range (µM)	LOD (µM)	Ref.
MWCNTs/GCE	5 - 80	1	[23]
Graphene-CS/GCE	1 - 550	0.75	[24]
Thermally reduced GO	-	-	[25]
P-rGO	5 - 90	2.62	[26]
Carbon dot/rGO	5 - 600	1	[27]
MWCNTs/multielectrode array	6 -600	6×10^{-7}	[28]
Tx – 100/GPCNTCPE	10 - 100	3.41	[29]
Ag@BaTiO3/rCF	6.66 - 131.67	38×10^{-8}	This work

fabricated electrode for RS detection with other electrodes is given in Table 1.

Conclusion

In this study, a fast, cost effective, simple, sensitive and reliable method has been suggested for the synthesis of silver nanoparticle stabilized on $BaTiO_3$/rCF nanocomposites. The decoration of $BaTiO_3$ nanoparticles on rCF was successfully achieved by hydrothermal method. Further, silver nanoparticles are decorated on $BaTiO_3$/rCF to obtain the final nanocomposite Ag@$BaTiO_3$/rCF, which is used for the electrochemical determination of Resorcinol. The modified GCE exhibit better detection ability and achieved a wide linear range of 6.66 – 131.67 µM after completing the optimization conditions. From the linear regression equation, the value of R^2=0.9824 and the slope value 0.7814 reveal that the electrochemical determination of RS is a typical adsorption - controlled process. Based on the efficacy of the present modified electrode, it is suggested that the same may be very well exploited for effective sensing of different pollutants in water.

References

1 Murugan E, Saranya S & Aswini A, *Indian J Chem,* 59A (2020) 1285.
2 Murugan E & Kalpana K, *Anal Chem,* 91 (2019) 5667.
3 Akhavan O, Bijanzad K & Mirsepah A, *RSC Ad*v, 4 (2014) 20441.
4 Li W, Chen M, Yang Y, Yuan D, Ren Y & Cai X, *J Appl Polym Sci,* 136 (2019) 47447.
5 Chang S J, Liao W S, Ciou C J, Lee J T & Li C C, *J Colloid Inter f Sci*, 329 (2) (2009)300.
6 Prado L R, De Resende N S, Silva R S, Egues S M S & Salazar-Banda G R, *Chem Eng Process: Process Intensif*, 103 (2016)12.
7 Sreekantan S, Noor A F M, Ahmad Z A, Othman R & West A, *J Mater Process Technol*, 195 (1-3)(2008) 171.
8 Liu Q, Vanmol K, Lycke S, Van Erps J, Vandenabeele P, Thienpont H & Ottevaere, H, *RSC Adv,* 10 (24) (2020) 14274.
9 Topçu E, *Mater Res Bullet*, 121 (2020) 110629.
10 Morimoto N, Kubo T &Nishina Y, *Sci Rep*, 6 (2016)1.
11 Khodari M, Mersal G A M, Rabie E M & Assaf H F, *Int J ElectrochemSci*, 13 (2018) 3460.
12 Huang L, Cao Y &Diao D, *Sensor Actuat B: Chem*, 305 (2020) 127495.
13 Murugan E, Rubavathy Jaya Priya A, Janaki Raman K, Kalpana K, Akshata C. R, Santhosh Kumar S and Govindaraju S, *J. Nanosci. Nanotechnol*, 19 (2019) 7596.
14 Tseng T W, Rajaji U, Chen T W, Chen S M, Huang Y C, Mani V & Jothi A I, *Ultrason Sonochem*, 69 (2020) 105242.
15 Ma B, Wang M, Tian D, Pei Y & Yuan L, *RSC Adv*, 5 (2015) 41639.
16 Zhang L, Li T, Ji X, Zhang Z, Yang W, Gao J & Dang A, *ElectrochimicaActa*, 252 (2017) 306.
17 Kothandan D, Jeevan Kumar R & Chandra Babu Naidu, *J Asian Ceram Soc*, 6 (2018) 1.
18 Alam S N, Sharma N & Kumar L, *Graphene*, 6 (2017) 1.
19 Thakur S, Thakur V, Kaur A & Singh L, *J Non-Cryst Solids*, 557 (2021) 120563.

20 Surmenev R A, Chernozem R V, Skirtach A G, Bekareva A S, Leonova L A, Mathur S & Surmeneva M A, *Ceram Int*, 47 (2020) 8904.
21 Madhan K &Murugaraj R, *J Sol-Gel Sci Technol*, 95 (2020) 11.
22 Zamfir L G, Puiu M & Bala C, *Sensors*, 20(22)(2020) 6443.
23 Ghoreishi S M, Behpour M, Hajisadeghian E & Golestaneh M, *Arab J Chem*, 9 (2016) 1563.
24 Yin H, Zhang Q, Zhou Y, Ma Q, Zhu L & Ai S, *Electrochim Acta*, 56 (2011) 2748.
25 Li S J, Qian C, Wang K, Hua B Y, Wang F B, Sheng Z H & Xia X H, *Sens Actuators B: Chem*, 174 (2012) 441.
26 Zhang H, Bo X & Guo L, *Sens Actuators B: Chem*, 220 (2015) 919.
27 Zhang W, Zheng J, Lin Z, Zhong L, Shi J, Wei C & Hu S, *Anal Methods*, 7 (2015) 6089.
28 Ngamchuea K, Tharat B, Hirunsit P & Suthirakun S, *RSC Adv*, 10 (2020) 28454.
29 Tigari G, Manjunatha J G, Raril C & Hareesha N, *Nov Appro Drug Des Dev*, 4 (2019) 1.